

L-valley electron g factor in bulk GaAs and AlAs

K. Shen,¹ M. Q. Weng,^{2,*} and M. W. Wu^{1,2,†}

¹Hefei National Laboratory for Physical Sciences at Microscale,
University of Science and Technology of China, Hefei, Anhui, 230026, China

²Department of Physics, University of Science and Technology of China, Hefei, Anhui, 230026, China
(Dated: February 2, 2022)

We study the Landé g -factor of conduction electrons in the L -valley of bulk GaAs and AlAs by using a three-band $\mathbf{k} \cdot \mathbf{p}$ model together with the tight-binding model. We find that the L -valley g -factor is highly anisotropic, and can be characterized by two components, g_{\perp} and g_{\parallel} . g_{\perp} is close to the free electron Landé factor but g_{\parallel} is strongly affected by the remote bands. The contribution from remote bands on g_{\parallel} depends on how the remote bands are treated. However, when the magnetic field is in the Voigt configuration, which is widely used in the experiments, different models give almost identical g -factor.

PACS numbers: 71.70.Ej, 85.75.-d, 73.61.Ey

The knowledge to electron g -factor of semiconductors is of fundamental importance to investigate the spin-related problems. In the past decades, a lot of investigations have been carried out to understand the material and structure dependence of the g -factor.^{1,2,3,4,5,6,7} Experimentally, g -factor can be measured through the measurement of Lamour frequency by the techniques such as time resolved Faraday/Kerr rotation,^{5,6} or through the measurement of the Zeeman splitting by electron spin resonance.⁷ Theoretical studies of the g -factor are carried out through various band structure calculations, such as $\mathbf{k} \cdot \mathbf{p}$ model, tight-binding model and the *ab initio* calculation.^{8,10,11} For zinc blende materials, most of the previous studies focus on the g -factors at Γ point. As recent investigations have been extended to the spin dynamics far away from equilibrium,^{10,12,13,14,15} the knowledge of g factor of higher valleys becomes important. For III-V semiconductors, the g -factor in the X -valley is believed to be close to the Landé factor of free electron, g_0 , regardless of the materials due to the large band gap and the vanishing of the spin splitting at the X -point.^{16,17} By using two-band $\mathbf{k} \cdot \mathbf{p}$ Kane-like model,^{16,18} it is shown that the g -factor in the vicinity of the L -valley of IV semiconductors is highly anisotropic and can be characterized by g_{\parallel} and g_{\perp} which correspond to the g -factor along the directions parallel and perpendicular to the L -axis (i.e., along $[111]$ direction for the $[111]$ valley). However, the investigations of g -factor in the L -valley of III-V semiconductors are still to be carried out, especially for GaAs ($\text{Ga}_{1-x}\text{Al}_x\text{As}$), one of the most promising materials for realizing the spintronic device.^{19,20,21,22,23,24} In this paper, we present the g -factor of the L -valley of GaAs and AlAs by $\mathbf{k} \cdot \mathbf{p}$ band structure calculation. With these two g -factors, one can further obtain the g -factor of $\text{Ga}_{1-x}\text{Al}_x\text{As}$ by linear interpolation on x , which is widely used in practice to get the material parameters of the semiconductor alloy.^{8,9,25}

Similar to the effective mass, the electron g -factor of a specific band is affected by the remote bands. The relevant bands in the vicinity of L -point in our calculation are shown in Fig. 1 and are identified by their symmetries.

The bands with L_3 symmetry split to bands with $L_{4,5}$ and L_6 symmetries due to the spin-orbit coupling. L_{1c} is the lowest conduction band at which we target. In addition to the top valence band L_{3v} included in the two-band Kane-like model,²⁶ we further include higher conduction bands L_{3c} as the gap between L_{3c} and L_{1c} bands is close to the gap between L_{3v} and L_{1c} in bulk GaAs/AlAs. In the calculation of g_{\perp} we also include the remote band L_{2c} . The other remote bands are neglected in the calculation since they are too far away from the conduction band to make any important effect.²⁷ For the general information of the band structure and the symmetry of zinc-blende materials, one can refer to the literature, say Ref. 28.

Follow the standard $\mathbf{k} \cdot \mathbf{p}$ calculation procedure, the anisotropic g factor of L_{1c} band can be expressed as²⁶

$$\mathbf{g} = g_0 \mathbf{1} + \frac{2}{m_0 i} \sum_{\mu\nu}' \frac{1}{(E_{L_{1c}} - E_{\mu})(E_{L_{1c}} - E_{\nu})} \{ \mathbf{h}_{0\mu} (\mathbf{p}_{\mu\nu} \times \mathbf{p}_{\nu 0}) + \mathbf{h}_{\mu\nu} (\mathbf{p}_{0\mu} \times \mathbf{p}_{\nu 0}) + \mathbf{h}_{\nu 0} (\mathbf{p}_{\nu 0} \times \mathbf{p}_{\mu\nu}) \}, \quad (1)$$

where $\mathbf{p}_{\mu\nu}$ is inter-band momentum matrix element between μ and ν bands. Noted that index “0” denotes L_{1c} band. \mathbf{h} is the effective magnetic field from the spin-orbit coupling. g_0 and m_0 are the Landé factor and mass of free electron. In the coordinate system defined by the principle axes of the constant energy conduction band ellipsoid, i.e. z -axis parallels to Γ - L axis, the g matrix is diagonal, with $g_{xx} = g_{yy} = g_{\perp}$ and $g_{zz} = g_{\parallel}$. The contribution of the remote band is reverse proportional to the band distance. Therefore, the closest bands have most significant effects. However, for g_{\perp} , there are no direct corrections from the closest L_{3v} and L_{3c} bands due to the symmetry. Instead, the corrections come from the indirect ones through the mediation of far-away remote bands.^{16,26} With the next closest L_{2c} band included, g_{\perp} reads,²⁶

$$g_{\perp} - g_0 = \text{Re} \frac{4}{m_0 i} \sum_{\mu} \frac{\langle L_{1c} | p_y | L_{3\mu} \rangle}{(E_{L_{1c}} - E_{L_{3\mu}})(E_{L_{1c}} - E_{L_{2c}})} \times \langle L_{3\mu} | h_x | L_{2c} \rangle \langle L_{2c} | p_z | L_{1c} \rangle. \quad (2)$$

TABLE I: Band structure parameters and g factors at L point for GaAs and AlAs. The rows labeled “ α ” and “ β ” represent the results from three-band model by choosing the value of λ to be corresponding value of L -point of Ge and the value at Γ -point.² The rows with “ γ ” denote the results from two-band model.

		$E_{L_{1c}}$ (eV)	$E_{L_{3v}}$ (eV)	$E_{L_{3c}}$ (eV)	δ (eV)	δ' (eV)	m_l (m_0)	m_t (m_0)	P (eVÅ)	P' (eVÅ)	g_{\perp}	g_{\parallel}	g_x
GaAs	α	1.85 ^a	-1.20 ^a	5.47 ^a	0.22 ^a	0.08	1.9 ^{a,b}	0.075 ^a	12.5	2.75	2.03	1.09	1.77
	β	1.85 ^a	-1.20 ^a	5.47 ^a	0.22 ^a	0.08	1.9 ^{a,b}	0.075 ^a	13.5	6.14	2.03	0.89	1.74
	γ	1.85 ^a	-1.20 ^a	5.47 ^a	0.22 ^a	0.08	1.9 ^{a,b}	0.075 ^a	12.2	0	2.03	1.14	1.78
AlAs	α	2.581 ^c	-0.983 ^c	5.069 ^c	0.208 ^c	0.058	1.9 ^{a,b}	0.096 ^{a,b}	11.9	2.62	2.03	1.41	1.85
	β	2.581 ^c	-0.983 ^c	5.069 ^c	0.208 ^c	0.058	1.9 ^{a,b}	0.096 ^{a,b}	15.0	8.00	2.03	0.93	1.74
	γ	2.581 ^c	-0.983 ^c	5.069 ^c	0.208 ^c	0.058	1.9 ^{a,b}	0.096 ^{a,b}	11.5	0	2.03	1.46	1.86

^aRef. 27; ^bRef. 29; ^cRef. 30

It is expected that this value is small due to the large gap between L_{1c} and L_{2c} bands. In order to calculate the contribution of the remote bands quantitatively, one needs the matrix elements of \mathbf{h} and \mathbf{p} which are not accessible theoretically by the $\mathbf{k} \cdot \mathbf{p}$ calculation alone. In practice, these elements can be obtained by fitting the experiment data, such as effective masses and band gaps. In the framework of the $\mathbf{k} \cdot \mathbf{p}$ theory, the anisotropic effective mass m^* of L -point is²⁶

$$\frac{m_0}{m^*} = 1 + \frac{2}{m_0} \sum_{\mu} \frac{\langle L_{1c} | \mathbf{p} | \mu \rangle \langle \mu | \mathbf{p} | L_{1c} \rangle}{E_{L_{1c}} - E_{\mu}}. \quad (3)$$

For the longitudinal mass,

$$\frac{m_0}{m_l} = \frac{m_0}{m_{zz}} = 1 + \frac{2}{m_0} \frac{|\langle L_{1c} | p_z | L_{2c} \rangle|^2}{E_{L_{1c}} - E_{L_{2c}}}. \quad (4)$$

The L_{3v} spin-orbit split off band gap $\delta = 2i\langle L_{3v} | h_z | L_{3v} \rangle$. By assuming that all the non-vanishing \mathbf{p} elements in Eq. (2) and (4) are the same, and all of the non-vanishing \mathbf{h} elements are equal to each other, g_{\perp} can be expressed as

$$g_{\perp} - g_0 \cong -\delta(m_0/m_l - 1)/(E_{L_{1c}} - E_{L_{3v}}). \quad (5)$$

Using the experiment data of m_l and δ , one can justify that the correction to g_{\perp} is rather small for both GaAs and AlAs due to the large gap between L_{1c} and L_{3v}/L_{2c} bands. Take GaAs as an example, $m_l/m_0 = 1.9$ while $\delta = 0.22$ eV is much smaller than the band gap (about 3 eV).^{27,29} As a result, g_{\perp} differs from g_0 by only 2%. The closeness of g_{\perp} to g_0 at L -point is not limited to GaAs but rather universal property of semiconductor with diamond and zinc-blende structures, in which the symmetry eliminates the direct correction from the closest bands.²⁶

The parallel component $g_{\parallel} = g_{zz}$ is very different. It reads²⁶

$$g_{\parallel} - g_0 = \text{Re} \frac{4}{m_0 i} \sum_{\mu\nu} \frac{\langle L_{1c} | p_x | L_{3\mu} \rangle}{(E_{L_{1c}} - E_{L_{3\mu}})(E_{L_{1c}} - E_{L_{3\nu}})} \times \langle L_{3\mu} | h_z | L_{3\nu} \rangle \langle L_{3\nu} | p_y | L_{1c} \rangle. \quad (6)$$

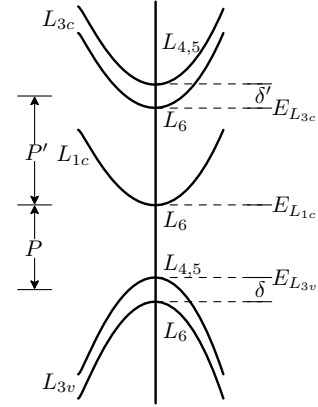


FIG. 1: Schematic of band structure near L point for zinc-blende crystal.

With the modifications from L_{3c} and L_{3v} bands, it can be written as¹⁶

$$g_{\parallel} - g_0 = -\frac{2m_0}{\hbar^2} [P^2 \frac{\delta}{E_g(E_g + \delta)} + P'^2 \frac{\delta'}{E'_g(E'_g + \delta')}] . \quad (7)$$

Here $E_g = E_{L_{1c}} - E_{L_{3v}}$ and $E'_g = E_{L_{3c}} - E_{L_{1c}}$ are the band gaps. δ' is the spin-orbit splitting of the L_{3c} conduction band. $-im_0P(P')/\hbar$ is the non-vanishing inter-band momentum matrix element between L_{1c} and L_{3v} (L_{3c}) bands. Among these parameters, the band gaps and the spin-orbit splittings can be measured directly or obtained through band structure calculations. In our calculation, we use the experiment data from Refs. 27 and 29 when available. For the parameters without experiment data, theoretical results from the tight-binding model are used.^{12,30} Since there is no value of δ' in the literature, we calculate it using the tight-binding model with the tight-binding parameters taken from Ref. 30. All the parameters in Eq. (7) are listed in Table I, except P and P' . However, there are neither direct experimental data nor theoretical results from three band model on P and

P' . In $\mathbf{k} \cdot \mathbf{p}$ band structure calculation, both are determined by fitting other experimentally measurable parameters. Here we use the transversal effective mass as a fitting target. From Eq. (3), the transversal effective mass $m_t = m_{xx}$ reads¹⁶

$$\frac{m_0}{m_t} - 1 = \frac{m_0}{\hbar^2} \left[P^2 \left(\frac{1}{E_g} + \frac{1}{E_g + \delta} \right) - P'^2 \left(\frac{1}{E_g} + \frac{1}{E_g + \delta'} \right) \right]. \quad (8)$$

Besides this, one more relation, i.e., P'/P , is required in order to obtain P and P' . There are three possible ways to estimate the value of $\lambda = P'/P$. The first is based on the assumption that this ratio at the same symmetry point is an universal constant for different materials.⁸ From the experiment data of Ge given in Refs. 16 and 27, i.e., $E_{L_{1c}} = 0.744$ eV, $E_{L_{3v}} = -1.53$ eV, $E_{L_{3c}} = 4.3$ eV, $\delta = 0.23$ eV, $\delta' = 0.27$ eV, $m_t = 0.0791m_0$ and $g_{\parallel} = 0.82$, we obtain $\lambda = 0.22$ at L -point from Eqs. (7) and (8).²⁵ With this value, one finds that $g_{\parallel} = 1.09$ and 1.41 for GaAs and AlAs respectively. This set of parameters are listed in Table I with rows labeled “ α ”. The second way is to assume that λ at different valleys are the same. In this way, we can use the value of λ at Γ -point where the band structure is well studied.² For GaAs (AlAs), $\lambda = 0.456$ (0.533), which give $g_{\parallel} = 0.89$ (0.93). These values are listed in Table I in the rows labeled “ β ”. The third way to choose λ is to set it to be zero and thus reduce the three-band model to two-band one.^{16,26} The corresponding results are shown in Table I with rows labeled “ γ ”. From the table, one can see that the remote bands have significant effect on g_{\parallel} . However, the contribution of the remote bands strongly depends on how the remote bands are treated. We comment that all the three estimations of λ above have their reasonings. However, one has no way to judge which one is the best without experiments. Fortunately, there is certain important case where the corresponding g -factor does not depend on the model one uses, which we address in the following.

From the table, one finds that g -factor in L -valley is highly anisotropic. When an applied magnetic field departs from the principle axis, the corresponding g -factor is a combination of g_{\perp} and g_{\parallel} . Moreover, different valleys also contribute differently. The overall g -factor should be averaged over the four L -valleys. However, when the magnetic field is along some highly symmetric crystal axis, such as $[100]$ direction (i.e., in Voigt configuration), all the four L -valleys have the same overall g -factor. In this case, the g -factor can be expressed as

$$g_x = \sqrt{(g_{\perp}^2 + g_{\parallel}^2 \sin^2 \theta + g_{\perp}^2 \cos^2 \theta)/2}, \quad (9)$$

with $\cos^2 \theta = 1/3$ for $[100]$ direction. g_x is also listed in Table I. One finds that the values of g_x obtained from the three different choices of λ are very close to each other. The difference in g_x given by different models is less than 5%, even though the difference in g_{\parallel} can be as large as 20-30%. The closeness of g_x from the three results is not a coincidence. One can see from Eq. (9) that under the Voigt configuration, the contribution of g_{\perp}^2 to g_x^2 is more than twice as that of g_{\parallel}^2 . Moreover, the remote bands have marginal effect on g_{\perp} . As a result, g_x is model insensitive. This result is of particular interest, since the applied magnetic field is exactly along the $[100]$ direction in the Voigt configuration, which is widely used in the Kerr rotation experiments.³¹ We believe that the obtained g_x is reliable in studying the spin dynamics in L -valley in Voigt configuration.

In summery, we have investigated the L -valley Landé g -factor in bulk GaAs and AlAs using a three-band $\mathbf{k} \cdot \mathbf{p}$ model. The parameters used in the calculation are from experiment data if available, or from the tight-binding calculation otherwise. The g -factor in the L -valley is highly anisotropic and can be characterized by two components: the transversal one g_{\perp} , corresponding for the magnetic field perpendicular to the L -axis, and the longitudinal one g_{\parallel} , for the magnetic field parallel to the L -axis. The transversal component is close to the free electron g -factor due to symmetry. Whereas the longitudinal component is shown to be strongly affected by the remote bands. The contribution of the remote bands depends on how these bands are treated, and the results are quite different. It is hard to judge which one is more reasonable without the justification of the experiments. However, when the magnetic field is in Voigt configuration (i.e., along $[100]$ axis) which is widely used in experiments investigating spin dynamics, different methods used in this investigation give almost identical Landé factors: $g_x \simeq 1.77$ for GaAs and 1.85 for AlAs.

This work was supported by the Natural Science Foundation of China under Grant Nos. 10574120 and 10725417, the National Basic Research Program of China under Grant No. 2006CB922005 and the Knowledge Innovation Project of Chinese Academy of Sciences.

* Electronic address: weng@ustc.edu.cn.

† Electronic address: mwwu@ustc.edu.cn.

¹ T. Ando, A. B. Fowler, and F. Stern, Rev. Mod. Phys. **54**, 437 (1982).

² R. Winkler, *Spin-Orbit Coupling Effects in 2D Electron*

and Hole Systems (Springer, Berlin, 2003).

³ R. M. Hannak, M. Oestreich, A. P. Heberle, W. W. Rühle, and K. Kohler, Solid State Commun. **93**, 319 (1995).

⁴ P. Le Jeune, D. Robart, X. Marie, T. Amand, M. Brousseau, J. Barrau, V. Kalevich, and D. Rodichev, Semi-

- cond. Sci. Technol. **12**, 380 (1997).
- ⁵ A. Malinowski and R. T. Harley, Phys. Rev. B **62**, 2051 (2000).
 - ⁶ J. M. Kikkawa and D. D. Awschalom, Phys. Rev. Lett. **80**, 4313 (1998).
 - ⁷ C. Weisbuch and C. Hermann, Phys. Rev. B **15**, 816 (1997).
 - ⁸ D. J. Chadi, A. H. Clark, and R. D. Burnham, Phys. Rev. B **13**, 4466 (1976).
 - ⁹ I. Vurgaftman, J. R. Meyer and L. R. Ram-Mohan, J. Appl. Phys. **89**, 5815 (2001).
 - ¹⁰ J. M. Jancu, R. Scholz, E. A. de Andrada e Silva, and G. C. La Rocca, Phys. Rev. B **72**, 193201 (2005).
 - ¹¹ M. Cardona, N. E. Christensen, and G. Fasol, Phys. Rev. B **38**, 1806 (1988).
 - ¹² J. Y. Fu, M. Q. Weng, and M. W. Wu, Physica E **40**, 2890 (2008).
 - ¹³ S. Saikin, M. Shen, and M.-C. Cheng, J. Phys.: Condens. Matter **18**, 1535 (2006).
 - ¹⁴ P. Zhang, J. Zhou, and M. W. Wu, Phys. Rev. B **78**, 235323 (2008).
 - ¹⁵ J.-M. Jancu, R. Scholz, G. C. La Rocca, E. A. de Andrada e Silva, and P. Voisin, Phys. Rev. B **70**, 121306 (2004).
 - ¹⁶ F. A. Baron, A. A. Kiselev, H. D. Robinson, K. W. Kim, K. L. Wang, and E. Yablonovitch, Phys. Rev. B **68**, 195306 (2003).
 - ¹⁷ A. A. Sirenko, T. Ruf, K. Eberl, M. Cardona, A. A. Kiselev, E. L. Ivchenko, and K. Ploog, in *High Magnetic fields in Semiconductor Physics*, edited by G. Landwehr and W. Ossau (World Scientific, Singapore, 1996), p.561.
 - ¹⁸ E. O. Kane, J. Phys. Chem. Solids **1**, 249 (1957).
 - ¹⁹ E. L. Ivchenko and A. A. Kiselev, Fiz. Tekh. Poluprovodn. **26**, 1471 (1992) [Sov. Phys. Semicond. **26**, 827 (1992)].
 - ²⁰ A. A. Kiselev, E. I. Ivchenko, and U. Rössler, Phys. Rev. B **58**, 16353 (1998).
 - ²¹ P. Pfeffer and W. Zawadzki, Phys. Rev. B **74**, 115309 (2006).
 - ²² P. Pfeffer and W. Zawadzki, Phys. Rev. B **74**, 233303 (2006).
 - ²³ M. de Dios-Leyva, E. Reyes-Gómez, C. A. Perdomo-Leiva, and L. E. Oliveira, Phys. Rev. B **73** 085316 (2006).
 - ²⁴ M. de Dios-Leyva, N. Porras-Montenegro, H. S. Brandi, and L. E. Oliveira, J. Appl. Phys. **99**, 104303 (2006).
 - ²⁵ C. Hermann and C. Weisbuch, Phys. Rev. B **15**, 823 (1977).
 - ²⁶ L. M. Roth, Phys. Rev. **118**, 1534 (1960).
 - ²⁷ *Semiconductors: Group IV Elements and III-V Compounds*, edited by O. Madelung, Landolt-Börnstein, New Series, Group III, Vol. 17, Pt. a (Springer-Verlag, Berlin, 1982); *Semiconductors: Intrinsic Properties of Group IV Elements and III-V, II-VI and I-VII compounds*, edited by O. Madelung, Landolt-Börnstein, New Series, Group III, Vol. 22, Pt. a (Springer-Verlag, Berlin, 1987); *Semiconductors-Basic Data*, edited by O. Madelung, (Springer-Verlag, Berlin, 1996).
 - ²⁸ P. Y. Yu and M. Cardona, *Fundamentals of Semiconductors*, 3rd ed., (Springer-Verlag, Berlin, 2003).
 - ²⁹ G. Klimeck, R. C. Bowen, and T. B. Boykin, and T. A. Cwik, Superlattices and Microstructures **27**, 519 (2000).
 - ³⁰ J.-M. Jancu, R. Scholz, F. Beltram, and F. Bassani, Phys. Rev. B **57**, 6493 (1998).
 - ³¹ *Semiconductor Spintronics and Quantum Computation*, ed. by D. D. Awschalom, D. Loss, and N. Samarth (Springer-Verlag, Berlin, 2002); I. Žutić, J. Fabian, and S. Das Sarma, Rev. Mod. Phys. **76**, 323 (2004); J. Fabian, A. Matos-Abiadue, C. Ertler, P. Stano, and I. Žutić, acta physica slovacica **57**, 565 (2007); and references therein.